Int. J. Solids Structures Vol. 20, No. 5, pp. 513 524, 1984
Printed in Great Britain.

0020 7683/84 $3.00 + .00
Pergamon Press Ltd.

A CONTACT PROBLEM FOR THE ELASTIC QUARTER SPACE

L. M. Keer, J. C. Lee and T. Mura
Department of Civil Engineering, Northwestern University, Evanston, IL 60201, U.S.A.

(*Received* 18 *April* 1983; *in revised form* 29 *July* 1983)

Abstract—The problem of the contact between a smooth, rigid indenter and an elastic quarter space is solved using integral transform techniques. The indenter can have an arbitrary plan form and can extend to the edge of the quarter space. Numerical results are given when a rigid, right-circular body is pressed into the top surface of the quarter space, while keeping its axis parallel to the surface and perpendicular to the edge.

INTRODUCTION

The problem of determining a Green's function for the elastic quarter plane or quarter space is complicated by the nonseparability of the boundary conditions. The only methods that appear to prove feasible for an effective solution are numerical ones. The case for normal loading was first investigated by Hetenyi[1], who used the alternating method and iteration to obtain an acceptable result. The method was also previously used by Hetenyi[2] to obtain a solution to the quarter plane problem. Gerber[3] used Hetenyi's basic algorithm to extend the investigation to the related frictionless contact problem and obtained accurate results, provided that the indenter was not located too close to the edge of the quarter space.

Recently, Keer *et al.*[4] reinvestigated Hetenyi's problem for a concentrated load on a quarter space. They applied a Fourier transform in the direction of the edge, and thereby reduced the considered problem to that of a quarter plane, having a transform variable as a parameter. Techniques similar to those used by Sneddon[5] for the elastic quarter plane were also used in the solution to the reduced problem. In addition to normal loading, concentrated shear loads parallel and perpendicular to the edge were investigated so that, in principle, loading of any type could be treated.

The present analysis deals with the related contact problem. Here, it is assumed that a rigid, frictionless indenter is pressed into an elastic quarter space. It is assumed that the indenter can have an arbitrary plan form and that the contact can extend to the edge. Such a contact problem for the elastic half space was solved by Ahmadi *et al.*[6] in their investigation of non-Hertzian contact problems. The key to their solution was the fact that Love's[7] solution for a rectangular "patch" was available that gave a complete descreption of the stress state within the half space. The displacement at the center of the "patch" could be calculated in closed form, and an integral equation was established, whose solution gave both the area of the contact and the magnitude of the pressures over all of the patches contained within the contact. The problem was solved by prescribing a load over an area (larger than the correct area) and finding the correct area and distribution of pressures by iteration.

A similar technique is used here. The Boussinesq concentrated load is integrated over an area to obtain the solution for a rectangular patch having a constant normal load. By using the results of Love's solution and by taking a Fourier transform along the edge, integral equations similar to those of Ref.[4] are obtained, giving the load and deflection for a single patch. Once the solution for a generic patch is obtained, then the method used in Ref.[6] can be applied to the edge loaded contact problem. It should be pointed out that special treatment is required to obtain results valid near the edge, and it appears that the method of Ref.[1] can be used only for the case that the contact does not extend to the edge.

METHOD OF SOLUTION

This analysis will consider the problem of the contact between a smooth, rigid body and an elastic quarter-space. In the investigation presented here the numerical scheme will be sufficiently general to include the case where the indenter extends to the *edge* of the quarter space. The solution technique will rely upon the methods of the previous papers[4, 6], and the reader is referred to them for some of the details not included here.

Formulation of smooth contact problem

The contact problem may be formulated by the following considerations. Let two bodies, 1 and 2, be initially in contact at point 0, which is along the x-axis of an x-y coordinate system in the common tangent plane (Fig. 1). Since the bodies are frictionless, only a normal load is assumed to act over the contact area Ω between the two bodies. the separation functions between the two bodies before contact and after contact are $f(x, y)$ and $e(x, y)$, respectively. The following conditions must be satisfied

$$N(x, y) \geq 0 \quad (x, y) \in \Omega \tag{1}$$

$$N(x, y) = 0 \quad (x, y) \notin \Omega \tag{2}$$

$$e(x, y) = 0 \quad (x, y) \in \Omega \tag{3}$$

$$e(x, y) \geq 0 \quad (x, y) \notin \Omega. \tag{4}$$

If two points on the z_1 and z_2 axes far from the contact region in the two bodies are brought together by a distance δ, which is the relative approach, then the distance of two points A, B (AB is parallel to the z-axis, the common normal of the two bodies) will change from $f(x, y)$ to $e(x, y)$ through the relation:

$$e(x, y) = f(x, y) + w_1 + w_2 - \delta, \tag{5}$$

where w_1 and w_2 are normal displacements of the two bodies at points A,B due to the force P_N.

If the body 1 is assumed to be *rigid*, we have that $w_1 = 0$; then, the displacement w_2 can be expressed as

$$w_2(x, y) = \iint_\Omega G(x, y; x', y')N(x', y')\,dx'\,dy', \tag{6}$$

where $G(x, y; x', y')$ is the displacement at point (x, y) due to a concentrated force at point (x', y') for the quarter space ($x \geq 0, z \geq 0$ in Fig. 2). The contact problem can be

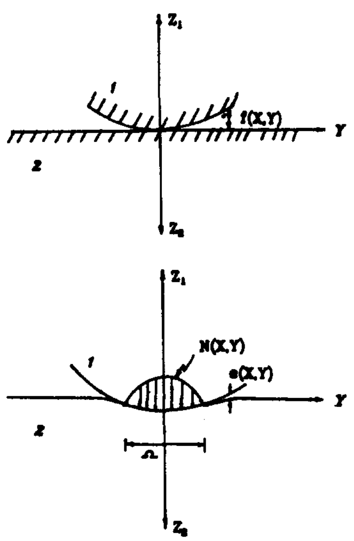

Fig. 1. Contact of two elastic bodies before and after the application of load.

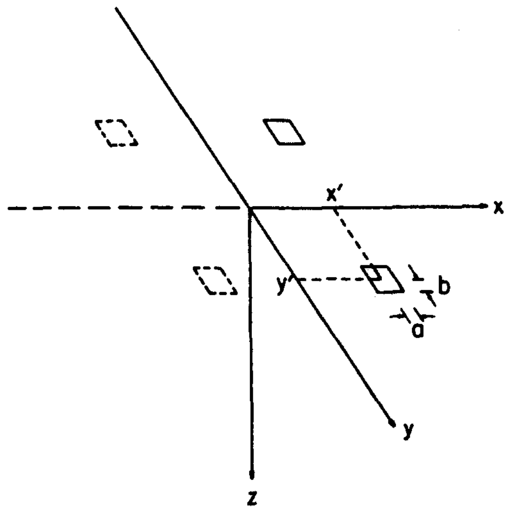

Fig. 2. Geometry and coordinates for quarter space.

formulated as follows:

$$e(x, y) = f(x, y) + \iint_{\Omega} G(x, y; x', y')N(x', y')\,\mathrm{d}x'\,\mathrm{d}y' - \delta. \quad (7)$$

By the definitions as given in eqns (1)–(4) for $(x, y) \in \Omega$, $e(x, y) = 0$, and eqn (7) becomes an integral equation with unknowns, $N(x, y)$, δ and Ω. By use of the equilibrium condition

$$\iint_{\Omega} N(x', y')\,\mathrm{d}x'\,\mathrm{d}y' = P_N, \quad (8a)$$

and by the inequality condition that

$$N(x, y) \geq 0 \text{ in } \Omega. \quad (8b)$$

A numerical method can be developed for the indentation of an elastic quarter space by a rigid indenter.

Suppose that $f(x, y)$ is symmetric with respect to the x-axis. If this is the case then $N(x, y)$ is also symmetric with respect to the x-axis, i.e. $N(x, y) = N(x, -y)$ and eqns (7) and (8) become

$$\iint_{\Omega'} [G(x, y; x', y') + G(x, y; x', -y')]N(x', y')\,\mathrm{d}x'\,\mathrm{d}y' = \delta - f(x, y)(x, y) \in \Omega' \quad (9)$$

and

$$\iint_{\Omega'} N(x', y')\,\mathrm{d}x'\,\mathrm{d}y' = P_N/2 \quad (10)$$

where Ω' is half of the contact area.

Numerical solution

The method of solution follows the numerical scheme given in Ref. [6]. The size of the contact region is overestimated, the resultant contact area is divided into rectangular patches, and the pressure over *each* patch is assumed to be constant. The integral in eqn (9) is subsequently evaluated over a generic rectangular region $2a \times 2b$, (see Fig. 2); this result produces a displacement at (x, y) equivalent to that due to the normal force $N_j = N(x', y')4ab$ applied to the patches whose centers are at (x', y') and $(x', -y')$.

The displacements caused by these two patches of traction can be obtained as in Ref.[1]. Image patches are put on at $(-x', y')$ and $(-x', -y')$ and the resulting normal stress $g(y, z)$ in the y-z plane are computed from Love's solution[7], Appendix 1. These stresses are removed by the previous algorithm[4]. The load-displacement relation on the surface for the half space can be obtained by integrating Boussinesq's solution, which is

$$\frac{1-\nu^2}{\pi E}\int_{x'-a}^{x'+a}\int_{y'-b}^{y'+b}\frac{\mathrm{d}u\,\mathrm{d}r}{\sqrt{(x-u)^2+(y-r)^2}} = \frac{1-\nu^2}{\pi E}[d(\bar{x}+a, \bar{y}+b)+d(\bar{x}-a, \bar{y}-b) - d(\bar{x}-a, \bar{y}+b)-d(\bar{x}+a, \bar{y}-b)] \quad (11)$$

where

$$d(r, s) = r\log(s+\sqrt{r^2+s^2}) + s\log(r+\sqrt{r^2+s^2}). \quad (12)$$

Here, $\bar{x} = x - x'$, $\bar{y} = y - y'$, E is Young's modulus, and ν is Poissòn's ratio.

The displacement due to the residual stress in the $y - z$ plane can be obtained as in the previous paper[4] and involves the solution of the following coupled integral equations:

$$\hat{p}(x, \beta) + \int_0^\infty K(x, \zeta; \beta)\hat{q}(\zeta, \beta)\,\mathrm{d}\zeta = 0 \quad 0 < x < \infty \quad (13)$$

$$\hat{q}(x, \beta) + \int_0^\infty K(x, \zeta; \beta)\hat{p}(\zeta, \beta)\,\mathrm{d}\zeta = \hat{g}(x, \beta) \quad 0 < x < \infty \quad (14)$$

where

$$K(x, \zeta; \beta) = \frac{2}{\pi}\left\{\frac{\beta^2 x\zeta^2}{x^2+\zeta^2}K_2(\beta\sqrt{x^2+\zeta^2}) - (1-2\nu)\left[\frac{\pi}{2}\beta\exp(-\beta\zeta) - \int_0^x \beta^2 K_0(\beta\sqrt{s^2+\zeta^2})\,\mathrm{d}s\right]\right\} \quad (15)$$

and

$$\hat{g}(x, \beta) = \int_{-\infty}^\infty g(x, y)\exp(i\beta y)\,\mathrm{d}y, \; \hat{p}(x, \beta) = \int_{-\infty}^\infty p(x, y)\exp(i\beta y)\,\mathrm{d}y. \quad (16)$$

Here, $K_0(s)$ and $K_2(s)$ are modified Bessel functions of the second kind with orders 0 and 2, respectively. Once the Fourier transforms $\hat{p}$ and $\hat{q}$ are solved from eqns (13) and (14), then the transformed displacement at the top surface (x-y plane) can be calculated as follows:

$$\hat{w}(x, \beta) = \frac{2(1-\nu^2)}{\pi E}\int_0^\infty \hat{p}(\zeta, \beta)[K_0(\beta(x+\zeta)) + K_0(\beta|x-\zeta|)]\,\mathrm{d}\zeta \equiv \frac{1-\nu^2}{\pi E}\hat{w}_0(x, \beta). \quad (17)$$

The displacement in terms of the x, y variables is

$$w(x, y) = \frac{1}{2\pi}\int_{-\infty}^\infty \hat{w}(x, \beta)\exp(-i\beta y)\,\mathrm{d}\beta = \frac{1-\nu^2}{\pi E}\left[\frac{1}{2\pi}\int_{-\infty}^\infty \hat{w}_0(x, \beta)\exp(-i\beta y)\,\mathrm{d}\beta\right]. \quad (18)$$

In the present example $g(x, y)$ is symmetric in the y-direction and the Fourier exponential transform is easily reduced to a Fourier cosine transform as

$$\hat{g}(x,\beta)=\frac{4\sin(\beta b)\cos(\beta y')}{\beta}\left\{-\frac{2}{\pi}\int_{x'-a}^{x'+a}\frac{\beta^2 x\zeta^2}{x^2+\zeta^2}K_2(\beta\sqrt{x^2+\zeta^2})\,d\zeta\right.$$

$$+(1-2v)\Bigg[\exp(-\beta(x'-a))-\exp(-\beta(x'+a))$$

$$\left.-\frac{2}{\pi}\beta^2\int_{x'-a}^{x'+a}\int_0^x K_0(\beta\sqrt{s^2+u^2})\,du\,ds\Bigg]\right\} \tag{19a}$$

$$\hat{g}(x,b)\equiv\frac{4\sin(\beta b)\cos(\beta y')}{\beta}\hat{g}_1(x,\beta). \tag{19b}$$

The double integral on the r.h.s. of (19) can easily be reduced to a single integral by transforming the variables into polar coordinates.

It is further noted that y' and b do not appear in $g_1(x,\beta)$. Let

$$\hat{p}(x,\beta\equiv\frac{4\sin(\beta b)\cos(\beta y')}{\beta}\hat{p}_1(x,\beta) \tag{20}$$

$$\hat{q}(x,\beta)\equiv\frac{4\sin(\beta b)\cos(\beta y')}{\beta}\hat{q}_1(x,\beta) \tag{21}$$

$$\hat{w}_0(x,\beta)\equiv\frac{4\sin(\beta b)\cos(\beta y')}{\beta}\hat{w}_1(x,\beta) \tag{22}$$

then the integral equations to be solved for are still eqns (13) and (14), but now $\hat{p}$, $\hat{q}$ and $\hat{g}$ are replaced by $\hat{p}_1$, $\hat{q}_1$ and $\hat{g}_1$, respectively. The displacement is written as follows:

$$w(x,y)=\frac{1-v^2}{\pi E}\frac{4}{\pi}\int_0^\infty\frac{\sin(\beta b)\cos(\beta y')\cos(\beta y)}{\beta}\hat{w}_1(x,\beta)\,d\beta. \tag{23}$$

For a series of patches with the same x' and a, the sets of integral equations needed to be solved are reduced to *one*.

Special consideration must be given to the case when $x'=a$ and the patches are to be calculated at the edge. For this case the transform $\hat{g}_1$ is split into two parts as

$$\hat{g}_1(x,\beta)=-2v\exp(-\beta x)+\frac{2}{\pi}\left\{\int_{x'+a}^{\infty}\frac{\beta^2x\xi^2}{x^2+\xi^2}K_2(\beta\sqrt{x^2+\xi^2})\,d\xi-(1-2v)\right.$$

$$\left.\times\int_{x'+a}^{\infty}\int_x^\infty K_0(\beta\sqrt{s^2+u^2})\,du\,ds\right\}. \tag{24}$$

The terms in the curly bracket decay exponentially for large β, but the first term will remain constant for small x. By substituting $\hat{g}_1(x,\beta)=-2v\exp(-\beta x)$ into eqn (14) and rearranging the integrand, one finds that β and x appear in pairs. Therefore,

$$\hat{p}_1(x,\beta)=\hat{p}_1(\beta x) \tag{25}$$

$$\hat{q}_1(x,\beta)=\hat{q}_1(\beta x) \tag{26}$$

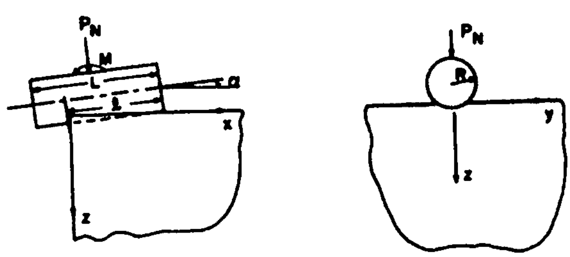

Fig. 3. Contact between cylinder and quater space: (a) side view, (b) front view.

and

$$\hat{w}_1(x,\beta)=2\int_0^\infty \hat{p}_1(\xi,\beta)[K_0(\beta(x+\xi))+K_0(\beta|x-\xi|)]\,d\xi$$
$$=\frac{2}{\beta}\int_0^\infty \hat{p}_1(\beta\xi)[K_0(\beta x+\beta\xi)+K_0(|\beta x-\beta\xi|)]\,d\beta\xi \tag{27a}$$
$$\hat{w}_1(x,\beta)\equiv\frac{1}{\beta}\hat{w}_1^*(\beta x). \tag{27b}$$

The portion of $w(x, y)$ due to $-2\nu\exp(-\beta x)$ for β larger than some value, say $1/(x'+a)$ can be obtained as

$$w(x,y)=\frac{1-\nu^2}{\pi E}\frac{4}{\pi}\int_{1/(x'+a)}^\infty \frac{\sin(\beta b)\cos(\beta y')\cos(\beta y)}{\beta}\hat{w}_1(x,\beta)\,d\beta$$
$$=\frac{1-\nu^2}{\pi E}\frac{4}{\pi}\int_{1/(x'+a)}^\infty \frac{\sin(\beta b)\cos(\beta y')\cos(\beta y)}{\beta^2}\hat{w}_1^*(\beta x)\,d\beta$$
$$=\frac{1-\nu^2}{\pi E}\frac{4}{\pi}\int_{x/(x'+a)}^\infty \frac{x\sin(\xi b/x)\cos(\xi y'/x)\cos(\xi y/x)}{\xi^2}\hat{w}_1^*(\xi)\,d\xi. \tag{28}$$

From eqn (17) it is seen that when $\beta\to 0$, the displacement $\hat{w}_1$ will be logarithmically singular. The displacement at the point 0 is

$$\hat{w}_1(0,\beta)=4\int_0^\infty \hat{p}_1(\xi,\beta)k_0(\beta\xi)\,d\xi. \tag{29}$$

If eqn (13) and (14) are multiplied by $K_0(\beta x)$, integrated with respect to x from 0 to infinity, and the following relation employed (see Appendix 2,[8]),

$$\int_0^\infty \frac{\beta^2 x\xi^2}{x^2+\xi^2}K_2(\beta\sqrt{x^2+\xi^2})K_0(\beta x)\,dx=K_0(\beta\xi) \tag{30}$$

then they can be written as

$$\int_0^\infty \hat{p}_1(x,\beta)K_0(\beta x)\,dx+\frac{2}{\pi}\int_0^\infty \hat{q}_1(x,\beta)K_0(\beta x)\,dx-(1-2\nu)\int_0^\infty H(x,\beta)\hat{q}_1(x,\beta)\,dx=0 \tag{31}$$

$$\int_0^\infty \hat{q}_1(x,\beta)K_0(\beta x)\,dx+\frac{2}{\pi}\int_0^\infty \hat{p}_1(x,\beta)K_0(\beta x)\,dx-(1-2\nu)\int_0^\infty H(x,\beta)\hat{p}_1(x,\beta)\,dx$$
$$=-\frac{2}{\pi}\int_{x'-a}^{x'+a}K_0(\beta x)\,dx+(1-2\nu)\int_{x'-a}^{x'+a}H(x,\beta)\,dx \tag{32}$$

where

$$H(x,\beta)=\frac{2}{\pi}\int_0^\infty K_0(s^2+\beta^2x^2)\left[\int_0^s K_0(t)\,dt\right]ds. \tag{33}$$

The integral involving $\hat{p}_1$ can be written as

$$\int_0^\infty \hat{p}_1(x,\beta)K_0(\beta x)\,dx=\frac{2\pi}{\pi^2-4}\int_{x'-a}^{x'+a}K_0(\beta x)\,dx+\frac{(1-2\nu)}{\pi^2-4}\left\{\int_0^\infty H(x,\beta)\right.$$
$$\left.\times[\pi\hat{q}_1(x,\beta)-2\hat{p}_1(x,\beta)]\,dx-\int_{x'-a}^{x'+a}H(x,\beta)\,dx\right\} \tag{34}$$

where the first term of the right-hand side would cause a singularity. However, the displacement due to this part will be (eqn 18):

$$w(0,y) = -\frac{1-\nu^2}{\pi E}\frac{8}{\pi(\pi^2-4)}\{h(y'+b+y)+h(y'+b-y)+h(y'-b+y)$$
$$+h(y'-b-y)\} \tag{35}$$

where

$$h(s) = \text{sign}\,(s)\{(x'-a)sh^{-1}(|s|/(x'-a)) - (x'+a)sh^{-1}(|s|/(x'+a))$$
$$-|s|sh^{-1}((x'+a)/|s|) + |s|sh^{-1}((x'-a)/|s|)\} \tag{36}$$

which is not singular and $sh^{-1}(s)$ is the inverse hyperbolic sine function.

In summary, the problem, therefore, is to solve eqns (9) and (10) where $N(x, y)$, δ and Ω' are unknown quantities. As mentioned earlier, the method of numerical solution follows the numerical scheme given in Ref.[6]. The size of the contact region is overestimated, the resultant contact area is divided into rectangular patches, and the pressure over each patch is assumed to be constant. The numerical solution can hence be obtained by replacing the integral equations by an appropriate set of simultaneous linear equations. Solving the equations, we find that some of the patches have negative pressure, and the sum of positive pressure should be greater than the total load. Those patches which have negative pressures are deleted and the equations are solved again until all patches have only positive pressures. This iteration scheme may be applied to other geometries if the load-surface displacement relation is known. For the present case the problem depends on the utilization of the quarter space solution[4].

The problem for the quarter space is formulated (as in [4]) by applying a Fourier transform to the loading and potentials in the direction of the edge of the quarter space. It is reduced to solving, eqns (13) and (14) and the other quantities are related to $\hat{p}$ and $\hat{q}$. In solving eqns (13) and (14), $\hat{p}$ and $\hat{q}$ are split into two parts, regular and singular. The resulting equations are solved numerically using 20-point Gauss–Legendre integration scheme. The infinite domain is transformed into the interval $(-1, 1)$ by the transformation $\xi = \tan(\pi(1+u)/4)$, which provides a finer mesh near the corner of the quarter space, where (1) the transforms $\hat{p}$ and $\hat{q}$ are functions that vary rapidly in the x and z directions and (2) the kernel has a high peak when both x and ξ are small. Some modification is made in order to avoid the high peak in the kernel. The same technique is applied in calculating the transformed surface displacement which has weak singularity at $x = \xi$ in eqn (17). To invert the displacement in eqn (18), a 26-point Gauss quadrature, in which an 11-point Radau Gaussian quadrature and a 15-point Gauss–Laguerre quadrature for the region $(0, 1)$ and $(1, \infty)$, were used.

EXAMPLE

An example is solved in which a rigid, right-circular cylinder (body 1) is pressed into the top surface of the quarter space, while keeping its axis parallel to the x-axis. The shape of the cylinder in the region of contact is assumed to be approximated by a parabola (Hertz approximation in the y-direction) as

$$f(x, y) = y^2/2R$$

where R is the radius of the cylinder (equal to 63.5 mm).

The material of the quarter space (body 2) is chosen to be steel with a Young's modulus of $E = 206.55$ GPA. The total normal load, P_N, is 1.3344×10^5 N. Poisson's ratio is allowed to vary; the results are shown in Figs. 4–6 for Poisson ratios of 1/6, 1/3 and 1/2, respectively. The trend shows clearly that as Poisson's ratio is increased, the region of contact near the edge becomes more narrow and the surface stress near the edge decreases in magnitude. For Poisson's ratio of 1/2 there is a distinct narrowing, when the distance from the edge is about equal to the contact width.

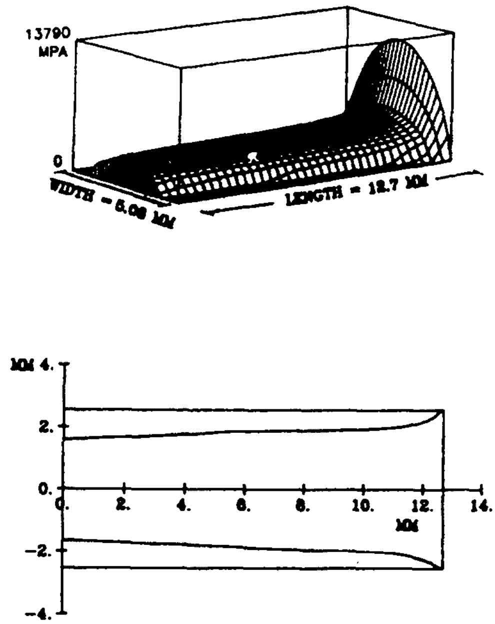

(a)

(b)

Fig. 4. Stress distribution for quater space indented by rigid right circular cylinder ($\nu = 1/6$, $\alpha = 0$): (a) stress distribution, (b) contact region.

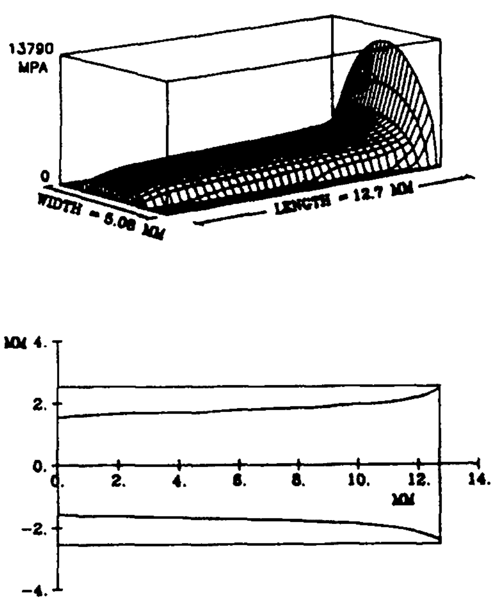

(a)

(b)

Fig. 5. Stress distribution for quarter space indented by rigid right circular cylinder ($\nu = 1/3$, $\alpha = 0$): (a) stress distribution, (b) contact region.

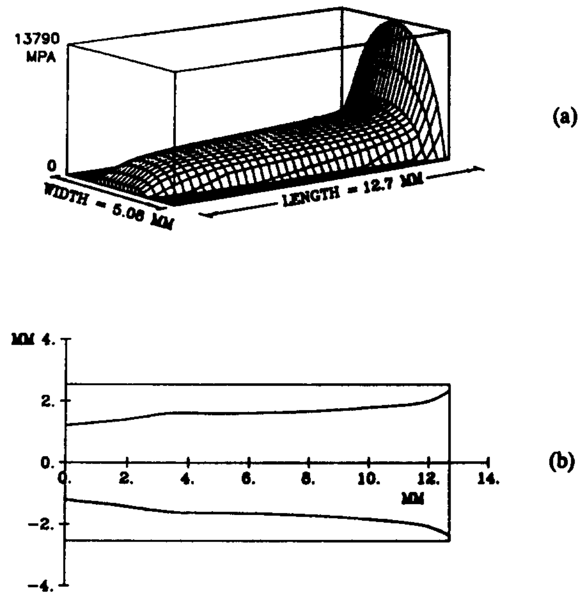

Fig. 6. Stress distribution for quarter space indented by rigid right circular cylinder ($\nu = 1/2$, $\alpha = 0$): (a) stress distribution, (b) contact region.

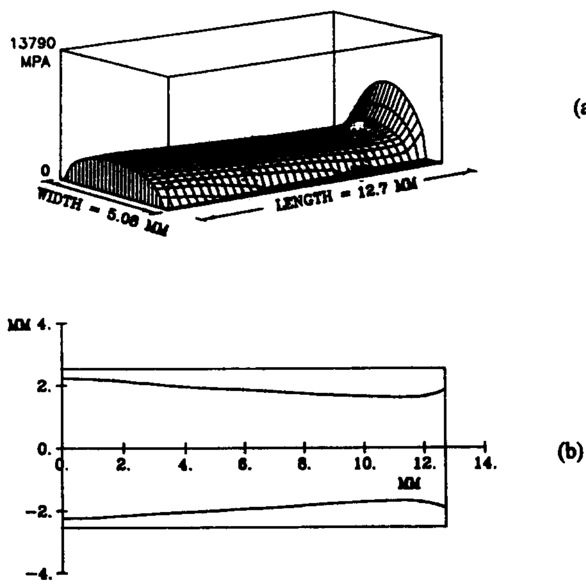

Fig. 7. Stress distribution for quarter space indented by rigid right circular cylinder ($\nu = 1/6$, $\alpha = 0.005$): (a) stress distribution, (b) contact region.

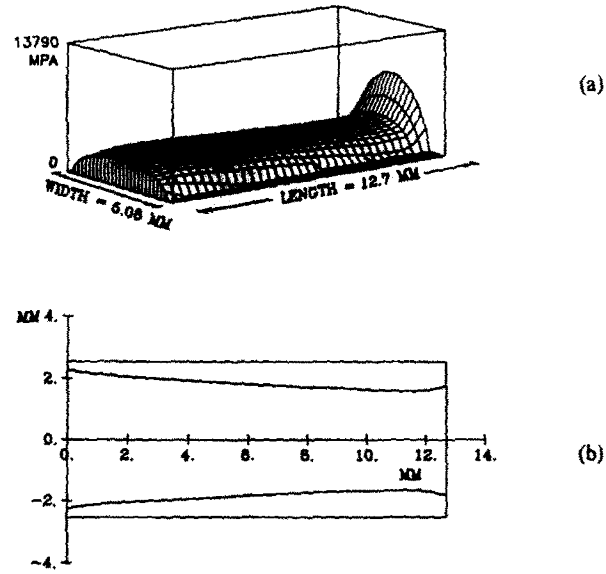

Fig. 8. Stress distribution for quarter space indented by rigid right circular cylinder ($\nu = 1/3$, $\alpha = 0.005$): (a) stress distribution, (b) contact region.

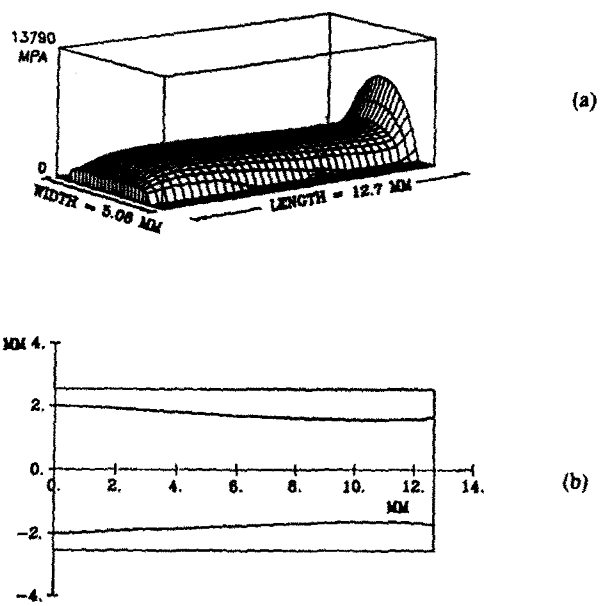

Fig. 9. Stress distribution for quarter space indented by rigid right circular cylinder ($\nu = 1/2$, $\alpha = 0.005$): (a) stress distribution, (b) contact region.

As a second example the cylinder axis is assumed to have a misalignment slope of 0.005 (angle = 0.005 radians). Although this example is for an inclined cylinder, the overall result is essentially the same (Figs. 7–9). As Poisson's ratio is increased, the contact footprint tends to decrease, relatively, near the edge; it has the smallest value at the edge for Poisson's ratio of 1/2. Also, the edge contact stress tends to decrease as the Poisson's ratio increases to 1/2.

Acknowledgement—The authors are grateful for support from the National Science Foundation, Grant CME7918015.

REFERENCES

1. M. Hetenyi, A general solution for the elastic quarter space, *J. Appl. Mech. Trans. ASME, Series E* **37**, 70–76 (1970).
2. M. Hetenyi, A method of solution for the elastic quarter plane. *J. Appl. Mech. Trans. ASME, Series E* **27**, 289–296 (1960).
3. C. E. Gerber, Contact problems for the elastic quarter plane and for the quarter space. Doctoral Dissertation, Stanford University (1968).
4. L. M. Keer, J. C. Lee and T. Mura, Hetenyi's elastic quarter space problem revisited. *Int. J. Solids Structures*, **19**, 497–508 (1983).
5. I. N. Sneddon, Fourier transform solution of quarter plane problems in elasticity. File No. PSR-9916, Applied Mathematics Research Group, North Carolina State University (1971).
6. N. Ahmadi, L. M. Keer and T. Mura, Non-Hertzian contact stress analysis—normal and sliding contact. *Int. J. Solids Structures*, **19**, 357–373 (1983).
7. A. E. H. Love, The stress produced in a semi-infinite solid by pressure on part of the boundary. *Phil. Trans. Royal Soc. London, Series A* **228**, 377–420 (1929).
8. A. Erdelyi (Ed.) *Table of Integral Transforms*. McGraw-Hill, New York (1954).

APPENDIX 1

$$g(y,z) = -\frac{1}{\pi}\{2\nu A + (1-2\nu)B - zC\}$$

where

$$\begin{aligned}A &= \tan^{-1}\frac{(a+x')(b-y+y')}{zR_1} + \tan^{-1}\frac{(a-x')(b-y+y')}{zR_2} + \tan^{-1}\frac{(a-x')(b+y-y')}{zR_3}\\ &+ \tan^{-1}\frac{(a+x')(b+y-y')}{zR_4} + \tan^{-1}\frac{(a+x')(b-y-y')}{zR_5} + \tan^{-1}\frac{(a-x')(b-y-y')}{zR_6}\\ &+ \tan^{-1}\frac{(a-x')(b+y+y')}{zR_7} + \tan^{-1}\frac{(a+x')(b+y+y')}{zR_8}\end{aligned}$$

$$\begin{aligned}B &= \tan^{-1}\frac{b-y+y'}{a+x'} + \tan^{-1}\frac{b+y-y'}{a+x'} + \tan^{-1}\frac{b-y+y'}{a-x'} + \tan^{-1}\frac{b+y-y'}{a-x'}\\ &+ \tan^{-1}\frac{b-y-y'}{a-x'} + \tan^{-1}\frac{b+y+y'}{a-x'} + \tan^{-1}\frac{b-y-y'}{a+x'} + \tan^{-1}\frac{b+y-y'}{a+x'}\\ &- \tan^{-1}\frac{z(b-y+y')}{(a+x')R_1} + \tan^{-1}\frac{z(b-y+y')}{(a-x')R_2} - \tan^{-1}\frac{z(b+y-y')}{(a-x')R_3} - \tan^{-1}\frac{z(b+y-y')}{(a+x')R_4}\\ &- \tan^{-1}\frac{z(b-y-y')}{(a+x')R_5} - \tan^{-1}\frac{z(b-y-y')}{(a-x')R_6} - \tan^{-1}\frac{z(b+y+y')}{(a-x')R_7} - \tan^{-1}\frac{z(b+y+y')}{(a+x')R_8}\end{aligned}$$

$$\begin{aligned}C &= \frac{a+x'}{(a+x')^2+z^2}\left(\frac{b-y+y'}{R_1} + \frac{b+y-y'}{R_4}\right) + \frac{a-x'}{(a-x')^2+z^2}\left(\frac{b-y+y'}{R_2} + \frac{b+y-y'}{R_3}\right)\\ &+ \frac{a+x'}{(a+x')^2+z^2}\left(\frac{b-y-y'}{R_5} + \frac{b+y+y'}{r_8}\right) + \frac{a-x'}{(a-x')^2+z^2}\left(\frac{b-y-y'}{R_6} + \frac{b+y+y'}{R_7}\right)\end{aligned}$$

$$R_1^2 = (a+x')^2 + (b-y+y')^2 + z^2 \quad R_5^2 = (a+x')^2 + (b-y-y')^2 + z^2$$

$$R_2^2 = (a-x')^2 + (b-y+y')^2 + z^2 \quad R_6^2 = (a-x')^2 + (b-y-y')^2 + z^2$$

$$R_3^2 = (a-x')^2 + (b+y-y')^2 + z^2 \quad R_7^2 = (a-x')^2 + (b+y+y')^2 + z^2$$

$$R_4^2 = (a+x')^2 + (b+y-y')^2 + z^2 \quad R_8^2 = (a+x')^2 + (b+y+y')^2 + z^2.$$

APPENDIX 2

We wish to prove that

$$\int_0^\infty \frac{\beta^2 x\xi^2}{x^2+\xi^2} K_2(\beta\sqrt{x^2+\xi^2})K_0(\beta x)\,dx = K_0(\beta\xi).$$

If Parseval's relation for Hankel transform is used, then

$$\begin{aligned}&\int_0^\infty \frac{\beta^2 x\xi^2}{x^2+\xi^2} K_2(\beta\sqrt{x^2+\xi^2})K_0(\beta x)\,dx\\ &= \beta^2\xi^2 \int_0^\infty x\left[\frac{K_2(\beta\sqrt{x^2+\xi^2})}{x^2+\xi^2}\right][K_0(\beta x)]\,dx\\ &= \beta^2\xi^2 \int_0^\infty y\left[\int_0^\infty x\frac{K_2(\beta\sqrt{x^2+\xi^2})}{x^2+\xi^2}J_0(xy)\,dx\right]\left[\int_0^\infty xK_0(\beta x)J_0(xy)\,dx\right]dy.\end{aligned}$$

Using the following identities[8]:

$$\int_0^\infty x \frac{K_2(\beta\sqrt{x^2+\xi^2})}{x^2+\xi^2} J_0(xy)\,\mathrm{d}x = \beta^{-2}\sqrt{\beta^2+y^2}K_1(\xi\sqrt{\beta^2+y^2})/\xi \quad \int_0^\infty xK_0(\beta x)J_0(xy)\,\mathrm{d}x = (\beta^2+y^2)^{-1}$$

we obtain

$$\int_0^\infty \frac{\beta^2 x\xi^2}{x^2+\xi^2} K_2(\beta\sqrt{x^2+\xi^2})K_0(\beta x)\,\mathrm{d}x = \xi \int_0^\infty \frac{y}{\sqrt{\beta^2+y^2}} K_1(\xi\sqrt{\beta^2+y^2})\,\mathrm{d}y = K_0(\beta\xi). \tag{30}$$